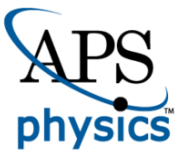

Calculated x-ray linear dichroism spectra for Gd-doped GaN

Tawinan Cheiwchanchamnangij and Walter R. L. Lambrecht

Phys. Rev. B **84**, 205119 — Published 15 November 2011

DOI: 10.1103/PhysRevB.84.205119

Calculated X-ray Linear Dichroism Spectra for Gd doped GaN.

Tawinan Cheiwchanchamnangij and Walter R. L. Lambrecht
Department of Physics, Case Western Reserve University, Cleveland, OH 44106-7079

Calculations of the X-ray linear dichroism (XLD) spectra of the Ga K-edge in GaN and the Gd L_3-edge in Gd doped GaN are presented. We show that these spectra can be modeled using partial densities of states standardly available in density functional band structure programs. We find good agreement with recent experiments for Gd on Ga site, showing that there is no need to invoke Gd on N or other sites to explain the spectra as previously claimed in the literature based on multiple scattering simulations.

I. INTRODUCTION

Gd doped GaN has attracted a lot of attention as a potential dilute magnetic semiconductor with "colossal" magnetic moments per Gd and ferromagnetic behavior above room temperature even for part per million concentrations of Gd.[1–6] Various spectroscopies have been used to study shed light on the origin of this very unusual magnetic behavior.[7–10] Recently, Ney et al.[11,12] presented X-ray Linear Dichroism (XLD) spectra of the Ga K-edge and the Gd L_3-edge and based on multiple scattering calculations of the latter concluded that Gd on Ga site alone could not account for the spectrum. They proposed that a significant fraction of the Gd (of order 15%) should be on antisites, i.e. on N sites. Furthermore, they claimed that the spectra showed evidence for the occurrence of Gd pairs on neighboring Ga substitutional and N antisites, showing incipient Gd clustering.

However, in a recent computational study,[13] we showed that the energy of formation for Gd on antisites is extremely high and makes this site very unlikely to occur under equilibrium conditions. We showed in fact that the Gd when forced to be on a N site is displaced toward interstitial sites by the very large size mismatch but even then has very high energy of formation. The same was true for Gd in Gd pairs. This previous study already casts serious doubts on this conjecture of Gd occurring on antisites.

Here we show that the XLD spectra can be modeled in terms of partial densities of states obtainable from a standard density functional band structure calculation and we show that good agreement is obtained with experiment for the expected Gd_{Ga} substitutional site.

II. COMPUTATIONAL METHOD

The XLD spectrum is simply the difference between the X-ray absorption spectrum (XAS) for two different polarizations. In other words, it measures the anisotropy of the XAS. Because of the dipole selection rule, for a Ga K-edge, XAS measures essentially the density of Ga p-like partial density of states (PDOS) in the conduction band assuming that the energy dependence of the matrix elements can be neglected. In an anisotropic material like wurtzite GaN and for measurements on the (0001) plane, the XLD spectrum corresponds to the difference between the p_z and $p_\perp$ Ga PDOS. These are straightforward to extract from a standard density functional theory (DFT) band structure calculation.

For the L_3 edge of Gd we essentially observe transitions from the Ga-2p core level to the Gd-5d and Ga-6s conduction band states. We can write the intensity for the spectrum for polarization β as:

$$I_\beta(E) = \sum_\alpha \sum_n^{unocc} \sum_{\mathbf{k}} |\langle L_\alpha | p_\beta | \psi_{n\mathbf{k}} \rangle|^2 \delta\left(E - (E_{n\mathbf{k}} - E_L)\right), \tag{1}$$

where L_α label the Cartesian components of the Gd-2p core-hole wavefunctions, E_L is the core-hole energy and $\psi_{n\mathbf{k}}$ and $E_{n\mathbf{k}}$ are the crystal eigenstates and band energies in a periodic boundary condition supercell model of the Gd doped GaN and p_β is the momentum matrix element. Decomposing the conduction band states into their local spherical harmonic expansion on Gd, we obtain,

$$\begin{aligned} I_\beta(E) &= \sum_\alpha \sum_n^{unocc} \sum_{\mathbf{k}} |\sum_{lm} \langle L_\alpha | p_\beta | \phi_{Gd,lm} \rangle \langle \phi_{Gd,lm} | \psi_{n\mathbf{k}} \rangle|^2 \\ &\quad \delta\left(E - (E_{n\mathbf{k}} - E_L)\right), \\ &\propto \sum_\alpha \sum_{lm} |\langle L_\alpha | p_\beta | \phi_{Gd,lm} \rangle|^2 N_{Gd,lm}(\omega), \end{aligned} \tag{2}$$

where, in the last step, we took the sum out of the absolute value, which amounts to an incoherent superposition, and we introduced the partial density of states $N_{Gd,lm}(\omega)$, with ω the energy above the conduction band minimum (CBM) which corresponds to the on-set of the spectrum. The dipole matrix element insures that we can have transitions only to Gd-6s or Gd-5d. We neglect the small Gd-6s contribution because only the d-states can have anisotropy. Assuming again that the energy dependence of the radial dipole matrix element between the core eigenstate and the Gd-d partial wave is negligible, the polarization dependence is captured by the factor

$$\int Y_{1\alpha}(\Omega) Y_{1\beta}(\Omega) Y_{2m}(\Omega) d\Omega \tag{3}$$

We here use the real or cubic harmonics. For parallel polarization, $\beta = z$ and for perpendicular polarization we pick $\beta = x$. Evaluating the few non-zero integrals between cubic harmonics and taking them modulo squared,

we obtain,

$$I_{\parallel} \propto \frac{3}{4}(N_{d_{xz}} + N_{d_{yz}}) + N_{d_{3z^2-r^2}},$$
$$I_{\perp} \propto \frac{3}{4}(N_{d_{xy}} + N_{d_{xz}} + N_{d_{x^2-y^2}}) + \frac{1}{4}N_{d_{3z^2-r^2}} \quad (4)$$

Finally, the XLD spectrum, $I_{\perp} - I_{\parallel}$, is given by

$$XLD \propto N_{d_{xy}} + N_{d_{x^2-y^2}} - N_{d_{yz}} - N_{d_{3z^2-r^2}}. \quad (5)$$

In the above, it is important that the z axis is chosen along the c-direction of the wurtzite unit cell and the spherical harmonics are accordingly defined.

We use the full-potential linearized muffin-tin orbital (FP-LMTO) method[14] for our band structure calculations. A 96-atom supercell is used to model Gd in wurtzite GaN. The positions of all the atoms are fully relaxed while the volume of the unit cell is kept that of pure GaN. The density functional theory is used in the local spin density approximation in the Barth-Hedin parameterization of exchange and correlation[15] and with Hubbard-U corrections for the Gd $4f$ orbitals,[16,17] i.e. the LSDA+U method. We use the fully localized limit (FLL) of the double-counting corrections in LSDA+U. The U-parameters for Gd are chosen as in GdN.[18] Because Gd has a half-filled 4f shell, only $U_f - J_f$ enters the Hamiltonian, where U_f is the screened on-site Coulomb interaction and J_f the exchange interaction. The parameter $U_f - J_f$ is chosen such that the Gd-$4f$ state splitting between occupied and empty states is in agreement with X-ray photoemission spectroscopy (XPS) and inverse photo-emission spectroscopy or Brehmstrahlung Isochromat Spectroscopy (BIS) for various Gd-pnictides.[19] A U_d parameter is also included as a way to shift up the Gd states slightly and adjust the band gap of GdN. These parameters have been used in several prior studies of GdN as well as Gd-doped GaN.[20,21] We use a $1 \times 1 \times 1$ k-point mesh to converge the charge densities during the structure relaxation and and a $2 \times 2 \times 2$ mesh with the tetrahedron method to obtain the PDOS.

III. RESULTS

First, we calculate the Ga K-edge XLD spectrum for pure GaN. The results are shown in Fig. 1 and compare quite well with the experimental spectrum measured for Gd containing sample, showing that the Ga is essentially unperturbed. The experimental spectrum was digitized from Fig. 1 in Ref.12.

We may note that even up to 30 eV above the CBM, where the LMTO method becomes somewhat less reliable because of the linearization in energy, the spectral shape is still well reproduced. The individual XAS for perpendicular and parallel polarization agree less well than the difference spectrum. Notably the experimental spectra show a higher intensity near the edge. This is due to the perturbation by the core-hole as is shown by comparing

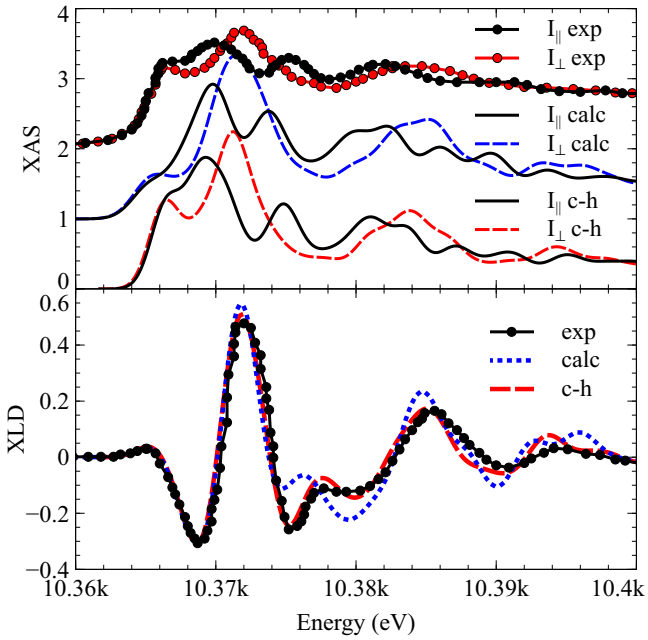

FIG. 1. XAS (above) and XLD (below) of Ga K-edge. The circles with lines are the experimental datas digitized from Ref.12, while the lines are the results from our calculations which include (c-h) and not include (calc) core-hole perturbation. The calculated XLD spectrum amplitude is scaled to match the depth of the first dip of the experimental spectrum. The energy axis is also shifted to match the position of the first dip, and the same amount of the energy shift is applied in the calculated XAS spectra.

also to calculations including the core-hole in an impurity type calculation. Interestingly, the effects of the core hole shift of intensity do not appear to be sensitive to the anisotropy so that even the unperturbed PDOS can be used to model the XLD.

Analyzing the first peaks in XAS at about 10 eV above the edge, we can see that the p_z or parallel PDOS show two peaks while the $p_{\perp}$ spectrum show one peak in the middle between the other two. This clearly explains the dip, peak, dip feature seen in the XLD. We can understand these features directly in terms of the local structure. The Ga-p_z orbitals have a different contribution to the bonds to N normal to the plane and mostly in the plane. The bond to the N atom right above the Ga should be stronger because the c/a is slightly lower than in the ideal tetrahedron. So, this corresponds to the upper peak in the $I_{\parallel}$ spectrum because these are antibonding states. The "in-plane" bonds are not completely in the xy-plane, so they still contribute a peak at lower energy in the $I_{\parallel}$ spectrum, in fact, a stronger peak because there are three of these. The $p_{\perp}$ orbitals on the other hand have no contribution to the bond normal to the plane and equal contribution to the other three bonds, so give rise to one peak. The feature at about 25 eV above the edge is less easy to explain in terms of Ga 4p states but we mainly notice an upward shift of the peak

in XAS from parallel to perpendicular polarization, resulting in a dip-peak structure in XLD. Furthermore, we learn that the Ga 4p like antibonding states are located at about 10 eV above the CBM.

Next, we show the calculated XLD spectrum for Gd substituted on Ga in GaN according to Eq. 5 in Fig. 2. Again, good agreement is obtained with the calculated spectrum, digitized from Fig. 2 in Ref. 12. A Gaussian broadening of 1.4 eV width is applied to the spectra. In this case, adding the core-hole appears to have negligible effect compared with the Ga K-edge spectrum. This is consistent with the fact that the Gd 2p states are less deep than the Ga 1s states. In particular, we note that our calculation reproduces the region above the first dip and peak between 7.25 keV and 7.26 keV in much better agreement with experiment than the multiple scattering theory (MST) calculations reported in Ref. 12. Those calculations obtain a big negative dip in this region inconsistent with the data. Even the broad peak between 7.26 and 7.27 keV is well reproduced. The main low energy features in the XLD are a dip at 7243 eV followed by a peak at 7248 eV. These features correspond to the Gd 5d like PDOS. The individual spectra for both polarizations both show two peaks but the first peak is higher in parallel and the second is higher in perpendicular polarization. We can ascribe these peaks to the e-symmetry and t_2-symmetry of the d-orbitals in a tetrahedral environment. Thus the e-states apparently become slightly more parallel polarized than the t_2-states.

Comparing with the individual PDOS shown in Fig. 3, we can see that the xy, yz, xz PDOS all look similar. We should however not confuse these with t_2-states because here we use x, y, z coordinates corresponding to the hexagonal structure, with z along the c-axis, i.e. pointing toward one of the tetrahedron corners, x parallel to one side of the tetrahedron, and y pointing toward another corner, where as the usual t_2 (e) states $x'y'$, $x'z'$, $y'z'$ ($3z'^2 - r'^2$, $x'^2 - y'^2$) correspond to cubic axes x', y', z' pointing toward the centers of the sides of the tetrahedron. Using the transformation between the two given by,

$$\begin{pmatrix} y_{xy} \\ y_{yz} \\ y_{3z^2-r^2} \\ y_{xz} \\ y_{x^2-y^2} \end{pmatrix} = \begin{pmatrix} 0 & \frac{\sqrt{2}}{3} & \frac{1}{\sqrt{3}} & 0 & -\frac{2}{3} \\ \frac{1}{\sqrt{3}} & -\frac{1}{3\sqrt{2}} & \frac{1}{\sqrt{3}} & -\frac{1}{\sqrt{6}} & \frac{1}{3} \\ 0 & -\sqrt{\frac{2}{3}} & 0 & 0 & -\frac{1}{\sqrt{3}} \\ -\frac{1}{\sqrt{3}} & -\frac{1}{3\sqrt{2}} & \frac{1}{\sqrt{3}} & \frac{1}{\sqrt{6}} & \frac{1}{3} \\ \frac{1}{\sqrt{3}} & 0 & 0 & \sqrt{\frac{2}{3}} & 0 \end{pmatrix} \begin{pmatrix} y_{x'y'} \\ y_{y'z'} \\ y_{3z'^2-r'^2} \\ y_{x'z'} \\ y_{x'^2-y'^2} \end{pmatrix}, \tag{6}$$

we can say for example that the real spherical harmonic y_{xy} contains 7/9 e-like states and 2/9 t_2-like states, y_{yz} and y_{xz} each contain 4/9 e-like states and 5/9 t_2-like states. The $y_{3z^2-r^2}$ has 1/3 e-like and 2/3 t_2-like contributions, and $y_{x^2-y^2}$ has pure t_2 character. In the PDOS we could somewhat arbitrarily ascribe the region below 10 eV as e-like and above 10 eV as t_2-like.This corresponds more or less to the crossing point between $I_\parallel$ and $I_\perp$ in the XAS spectrum or the zero crossing between the first major dip and peak in the XLD. The major origin for the higher $I_\parallel$ in the e-region is then the stronger contribution of the $3z^2 - r^2$ PDOS, which has a strong peak at 8 eV above the edge. Since this is a d-orbital combination pointing straight toward the apex tetrahedron corner in the c-direction, it makes sense that both peaks in this PDOS are pushed up relative to the other orbitals.

In the analysis of Ref.[12], the magnitude of the first dip to peak change in the Gd L_3 spectrum was found to be underestimated compared to the MST simulation for Gd on Ga site. The authors therefore added spectra for Gd on a N antisite. For the N on the antisite, the peak near this energy is weak and hence mixing in a certain amount of N on antisite spectra can adjust the peak height. However, any other spectrum with negligible anisotropy in this region would do the same, e.g. GdN which is isotropic or pure Gd. Thus the evidence for Gd on antisites is pretty weak. The present calculations show that good agreement with the experimental spectrum is already obtained with only Gd on Ga site and furthermore, our previous calculations indicated that Gd on N site is very unlikely.

IV. CONCLUSION

In conclusion, we have shown that XLD spectra can be well simulated in terms of standard PDOS. For K-edge spectra in anisotropic materials, this simply requires us to subtract in plane and out of plane p-like PDOS. For L_3-spectra, we have presented a spherical harmonic analysis which leads to a slightly more complicated combination of various d-like PDOS. Good agreement is obtained for the XLD spectrum even up to 30-40 eV above the edge in spite of using a linearized band structure method. For the specific case of Gd in GaN, we showed that there is no evidence for Gd on any other site than Ga substitutional. Finally, our analysis in terms of PDOS provides some additional insights in the nature of the XLD features.

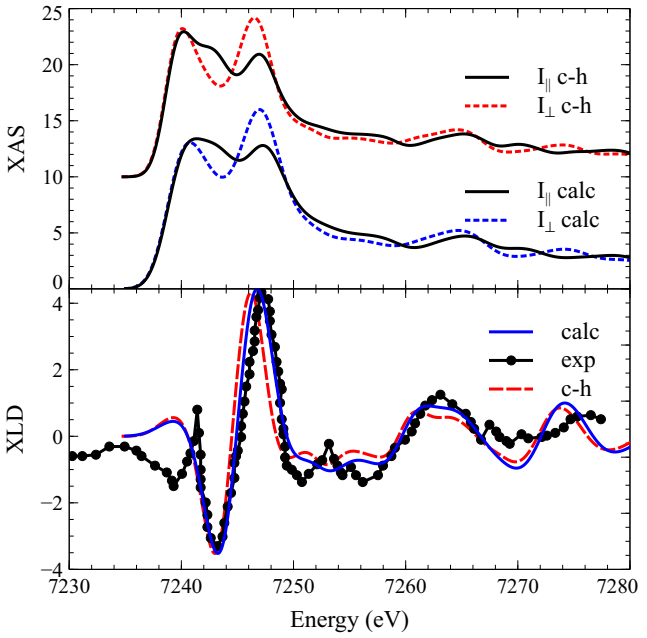

FIG. 2. XAS (above) and XLD (below) of Gd L_3-edge for Gd substituted on Ga in GaN. The circles with lines are the experimental datas digitized from Ref.12, while the lines are the results from our calculations which include (c-h) and not include (calc) core-hole perturbation. The experimental XLD spectrum amplitude is scaled and shifted down to match the depth of the first dip of the calculated datas. The energy axis is shifted to match the position of the first dip, and the same amount of the energy shift is applied in the calculated XAS spectra.

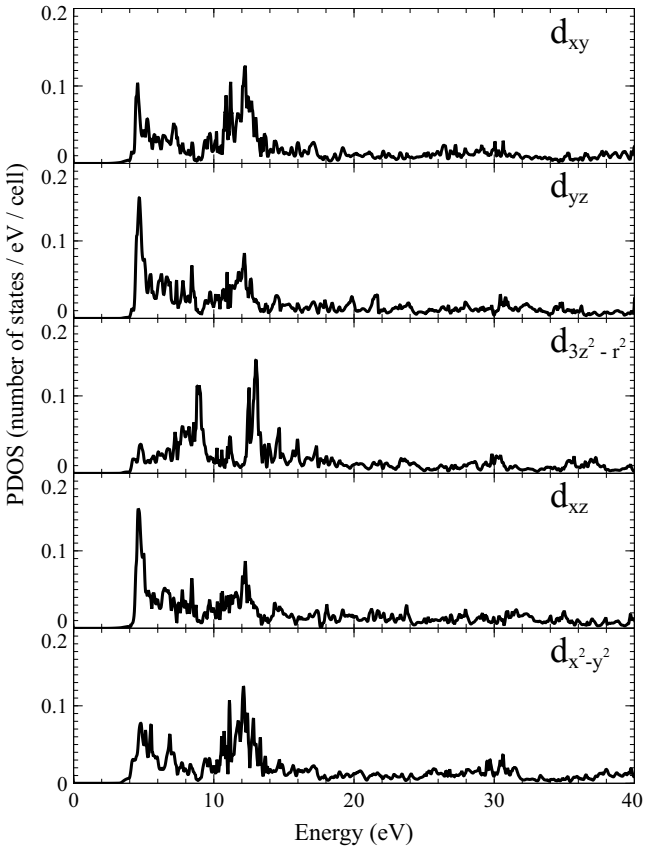

FIG. 3. PDOS of Gd d-orbitals calculated from Gd substituted on Ga in GaN supercell.

ACKNOWLEDGMENTS

This work made use of the High Performance Computing Resource in the Core Facility for Advanced Research Computing at Case Western Reserve University and the Ohio Supercomputer Center. The work was supported by the National Science Foundation under grant No. DMR-0710485.

[1] N. Teraguchi, A. Suzuki, Y. Nanishi, Y.-K. Zhou, M. Hashimoto, and H. Asahi, Solid State Commun. **122**, 651 (2002).

[2] H. Asahi, Y. K. Zhou, M. Hashimoto, M. S. Kim, X. J. Li, S. Emura, and S. Hasegawa, Journal of Physics: Condensed Matter **16**, S5555 (2004).

[3] S. Dhar, O. Brandt, M. Ramsteiner, V. F. Sapega, and K. H. Ploog, Phys. Rev. Lett. **94**, 037205 (2005).

[4] S. Dhar, L. Pérez, O. Brandt, A. Trampert, K. H. Ploog, J. Keller, and B. Beschoten, Phys. Rev. B **72**, 245203 (2005).

[5] L. Pérez, G. S. Lau, S. Dhar, O. Brandt, and K. H. Ploog, Phys. Rev. B **74**, 195207 (2006).

[6] M. A. Khaderbad, S. Dhar, L. Pérez, K. H. Ploog, A. Melnikov, and A. D. Wieck, Appl. Phys. Lett. **91**, 072514 (2007).

[7] A. Ney, T. Kammermeier, E. Manuel, V. Ney, S. Dhar, K. H. Ploog, F. Wilhelm, and A. Rogalev, Appl. Phys. Lett. **90**, 252515 (2007).

[8] T. Kammermeier, S. Dhar, V. Ney, E. Manuel, A. Ney, K. H. Ploog, F.-Y. Lo, A. Melnikov, and A. D. Wieck, Phys. Stat. Solidi (a) **205**, 1872 (2008).

[9] W. Gehlhoff, B. Salameh, and A. Hoffmann, Phys. Stat. Solidi (a) **1-4** (2011).

[10] M. Roever, J. Malindretos, A. Bedoya-Pinto, A. Rizzi, C. Rauch, and F. Tuomisto, Phys. Rev. B **84**, 081201 (2011).

[11] A. Ney, T. Kammermeier, K. Ollefs, V. Ney, S. Ye, S. Dhar, K. H. Ploog, M. Röver, J. Malindretos, A. Rizzi, F. Wilhelm, and A. Rogalev, J. Magn. Magn. Mater. **322**, 1162 (2010).

[12] A. Ney, T. Kammermeier, E. Manuel, V. Ney, S. Dhar, K. H. Ploog, F. Wilhelm, and A. Rogalev, Appl. Phys. Lett. **90** (2007).

[13] T. Cheiwchanchamnangij, A. Punya, and W. R. L. Lambrecht, MRS Proceedings **mrsf10-1290-i03-04** (2010), 10.1557/opl.2011.382.

[14] M. Methfessel, M. van Schilfgaarde, and R. A. Casali, in *Electronic Structure and Physical Properties of Solids. The Use of the LMTO Method*, Lecture Notes in Physics, Berlin Springer Verlag, Vol. 535, edited by H. Dreyssé (2000) p. 114.

[15] U. von Barth and L. Hedin, J. Phys. C: Solid State Phys. **5**, 1629 (1972).

[16] V. I. Anisimov, J. Zaanen, and O. K. Andersen, Phys. Rev. B **44**, 943 (1991).

[17] A. I. Liechtenstein, V. I. Anisimov, and J. Zaanen, Phys. Rev. B **52**, R5467 (1995).

[18] P. Larson, W. R. L. Lambrecht, A. Chantis, and M. van Schilfgaarde, Phys. Rev. B **75**, 045114 (2007).

[19] H. Yamada, T. Fukawa, T. Muro, Y. Tanaka, S. Imada, S. Suga, D.-X. Li, and T. Suzuki, J. Phys. Soc. Japan **65**, 1000 (1996).

[20] C. Mitra and W. R. L. Lambrecht, Phys. Rev. B **80**, 081202 (2009).

[21] C. Mitra and W. R. L. Lambrecht, Phys. Rev. B **78**, 134421 (2008).